CHEMBIOCHEM

DOI: 10.1002/cbic.200800036

Influence of δ-Functional Groups on the Enantiorecognition of Secondary Alcohols by *Candida antarctica* Lipase B

Jonas Nyhlén,[a] Belén Martín-Matute,[a] Anders G. Sandström,[a] Marco Bocola,*[b] and Jan-E. Bäckvall*[a]

The selectivity of acetylation of δ-functionalized secondary alcohols catalyzed by Candida antarctica *lipase B has been examined by molecular dynamics. The results from the simulation show that a δ-alcohol functionality forms a hydrogen bond with the carbonyl group of Thr40. This interaction stabilizes the tetrahedral intermediate and thus leads to selective acetylation of the* R *enantiomer. A stabilizing interaction of the δ-(*R*)-acetoxy group with the peptide NH of alanine 282 was also observed. No stabilizing interaction could be found for the δ-keto functionality, and it is proposed that this is the reason for the experimentally observed decrease in enantioselectivity. From these results, it was hypothesized that the enantioselectivity could be restored by mutating the alanine in position 281 for serine. The mutation was made experimentally, and the results show that the* E *value increased from 9 to 120.*

Introduction

The development of efficient methods for the synthesis of enantiomerically pure chiral molecules is of tremendous importance. In 2004, for example, it was reported that the active ingredients in nine of the top ten drugs produced were enantiomerically pure chiral molecules.[1] Pharmaceuticals containing only one enantiomer, the active drug, offer the possibility of being administered in a lower dosage, therefore minimizing side effects. New synthetic methods that control the stereochemistry in a molecule are of great importance not only for the synthesis of pharmaceuticals, but also for the synthesis of flavor and aroma chemicals, agricultural chemicals, and specialty materials.[2] Synthetic routes to produce these compounds have therefore emerged as one of the most important fields of organic chemistry.[2] Despite the growing number of available methods for the preparation of enantiomerically pure compounds, kinetic resolution (KR) is still the most widely employed method in industry,[3] and in most cases biocatalysts (enzymes) are used.

A KR is the total or partial separation of two enantiomers from a racemic mixture.[4] A KR is based on the different reaction rates of the enantiomers with a chiral molecule (a reagent, a catalyst, etc). In the ideal case, the difference is large, with one of the enantiomers reacting very rapidly to give the product, whereas the other either does not react at all or reacts very slowly and can be recovered enantiomerically pure when the transformation is completed (Scheme 1).

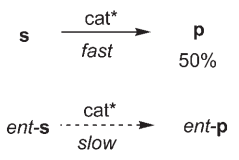

Scheme 1. Kinetic resolution (s: substrate, p: product, cat*: homochiral catalyst).

Candida antarctica lipase B (CALB) is among the most enantioselective lipases toward secondary alcohols, and its substrate specificity is very broad. In hydrolysis/synthesis of esters (lipase substrate type III; the chirality resides at the alcoholic center), CALB follows Kazlauskas' rule that predicts an enantiopreference for the *R* alcohol (Figure 1).[5]

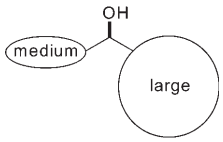

Figure 1. Empirical model for predicting the rapidly reacting enantiomer of a *sec*-alcohol.

The catalytic mechanism of triacylglycerol hydrolases, as well as serine proteases, involves the interaction of three amino acid residues: a nucleophilic serine, a histidine, and either an aspartate or a glutamate (Scheme 2). In the case of CALB, this catalytic triad consists of Ser105, His224, and Asp187. The charged tetrahedral intermediate is stabilized by the two backbone amide groups of Gln106 and Thr40, and additionally by the hydroxy group of the Thr40 side chain. The binding site is narrow and provides a small enantiorecognition pocket for secondary alcohols delineated by Thr42, Ser47, and Trp104.[6]

The first X-ray crystal structure of CALB was solved without any bound substrate.[7] Subsequently, two other low-resolution structures were also solved, one in complexation with an ester

[a] *J. Nyhlén, Dr. B. Martín-Matute, A. G. Sandström, Prof. J.-E. Bäckvall*
Department of Organic Chemistry, Arrhenius Laboratory
Stockholm University, 106 91 Stockholm (Sweden)
Fax: (+46) 8-154908
E-mail: jeb@organ.su.se

[b] *Dr. M. Bocola*
Department of Physical Biochemistry 2
Universitaetsstrasse 31, 93053 Regensburg (Germany)
Fax: (+49) 941-943-2813
E-mail: marco.bocola@biologie.uni-regensburg.de

Supporting information for this article is available on the WWW under http://www.chembiochem.org or from the author.

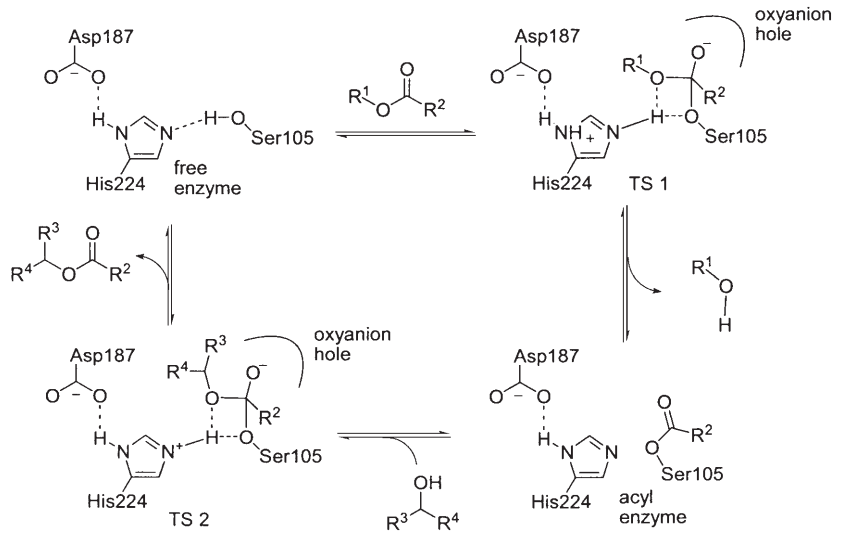

Scheme 2. Reaction mechanism of serine hydrolases. The esterification or transesterification involves two transition structures—TS1 and TS2—and one acyl enzyme intermediate.

substrate and the other with a covalently bound tetrahedral phosphonate.[8] These X-ray structures have provided the basis for several modeling studies. The enantiorecognition of chiral secondary alcohols by CALB has previously been investigated by minimization techniques[9] and molecular dynamics.[10] There is also a modeling study of secondary amines based on X-ray structures of CALB in complexation with (*R*)- and (*S*)-phenylethylamine-phosphonates.[11]

Despite the usual high enantioselectivity of CALB towards *sec*-alcohols, we have previously observed dramatic decreases in selectivity in the cases of certain secondary alcohols bearing keto or acetoxy groups a few carbons away from the carbinol to be acetylated.[12] Loss of selectivity occurs in spite of the fact that the steric bulk of the large group (vide supra, Figure 1) is essentially unchanged. Interestingly, very high selectivities are obtained for similar substrates not possessing any functional group,[13] as well as for those possessing a hydroxy group instead.[12,14] For example, the kinetic asymmetric transformations (KATs) of diastereomeric mixtures of diols **1** and **2** (Scheme 3) proceed in both cases with *pseudo E*[15] values of over 200, but if the δ-hydroxy groups are changed to keto groups (**3** and **4**) the *E* values drop to 9[12c] and 2.2,[12b] respectively.

Similar loss of selectivity has been observed in the consecutive acetylations of diols **5** (Scheme 4): whereas the KR of *rac*-**5** and the desymmetrization of *meso*-**5** to yield the corresponding monoacetates occur with very high selectivities ($E>200$), the acetylations from monoacetates **6** to yield diacetates are not so selective. In the KR of a racemic mixture of (*R*,*R*)-**6** and (*S*,*S*)-**6** there is still a large difference between the enantiomers, and the enzyme has a higher preference for the former ($E=94$). However, the KR of a racemic mixture of (*R*,*S*)-**6** and *ent*-(*R*,*S*)-**6**, derived from *meso*-**5**, proceeds with very low selectivity ($E=7$; Scheme 4).[12c]

Molecular dynamics (MD) simulation of the tetrahedral intermediate has previously been applied to estimate reactivities and enantioselectivities in the cases of CALB,[9–10] *Pseudomonas aeruginosa*,[16] *Pseudomonas cepacia*,[17] and *Bacillus subtilis*.[18]

In the work reported herein, we used MD simulations to study CALB enantiorecognition of a variety of *sec*-alcohols bearing alcohol, keto, or acetoxy groups in the δ-positions of the alcohols undergoing enzyme-catalyzed esterification. A model that is able to explain the experimental observations should provide us with a better understanding of the impor-

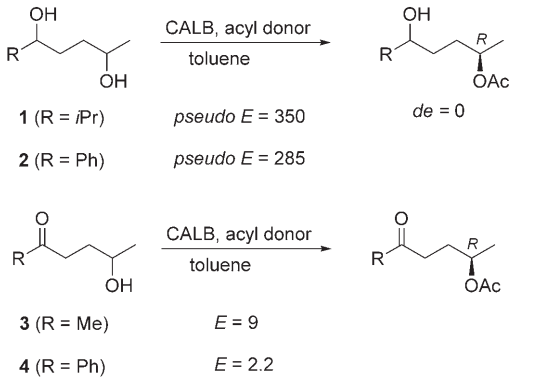

Scheme 3. CALB-catalyzed KATs of diols **1** and **2** and KRs of γ-hydroxyketones **3** and **4**.

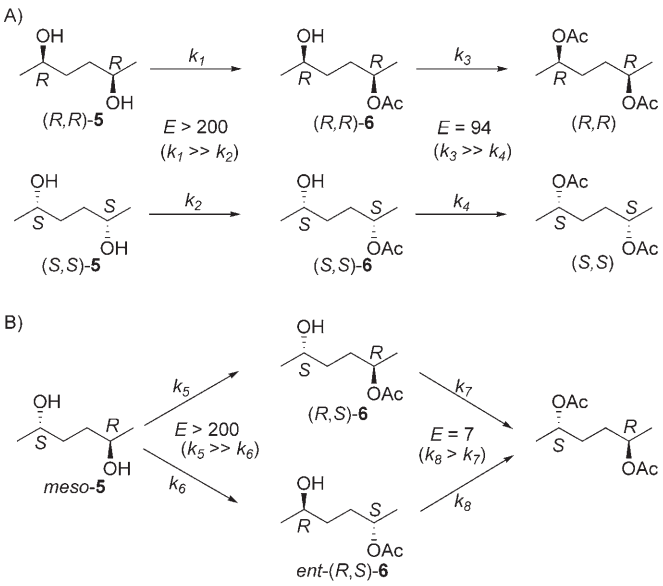

Scheme 4. Experimentally determined *E* values of CALB-catalyzed sequential esterification of A) *rac*-**5**, and B) *meso*-**5** in toluene.

tant features that govern the CALB-catalyzed acetylation reactions of functionalized substrates.

Results and Discussion

We have performed a modeling study of the enantioselectivity of CALB in complexation with secondary alcohols possessing hydroxy, acetate, or keto groups in the δ-positions relative to the alcohol moieties undergoing acetylation by the enzyme. The tetrahedral intermediates of the acetylation/deacetylation reactions are mainly stabilized by the backbone peptide and the hydroxy group of the Thr40 side chain. Thr40 thus plays a central role for the activity of the enzyme, and its importance has previously been investigated by Hult and colleagues.[19] Located in the small selectivity pocket, Thr40 creates a pocket for

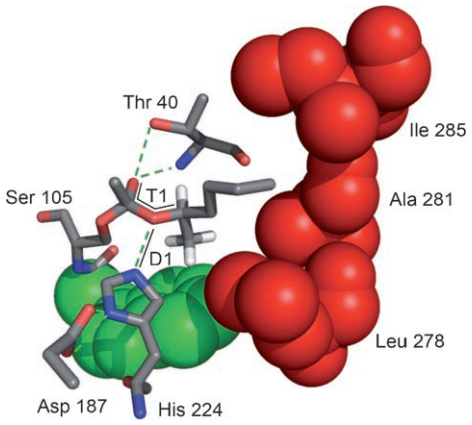

Figure 2. Stereospecificity pockets of CALB with hexan-2-ol as substrate. For clarity, only the α-hydrogen on the substrate and the hydrogen atoms on the 2-methyl group are shown. The large pocket, shown in red, points towards the entrance of the enzyme and holds the large substituent. The methyl group in the 2-position points down into the medium pocket, the size of which is limited by Trp104, shown in green. The α-hydrogen on the chiral center resides in a small pocket limited by Thr40, which also helps to stabilize the oxyanion by donating two hydrogen bonds. The figure shows the two most important descriptors: the dihedral angle T1, which governs the interaction with the medium pocket, and the distance D1, which governs the hydrogen bond distance between the substrate alcohol and His224.

the α-hydrogen atoms of (2*R*) substrates (Figure 2), whereas for the more slowly reacting (2*S*) substrates these same hydrogen atoms point in the opposite direction (mirror image conformation, as denoted by Kazlauskas and co-workers).[20] Furthermore, the carbonyl group of the Thr40 backbone introduces a hydrogen bond acceptor that can interact with the δ-functional groups on the substrates. According to our simulations, it can, for example, form hydrogen bonds to alcohol groups in δ-positions. These specific interactions seem to have a dramatic impact on the selectivity.

Several individual 1 ns MD simulations for all diastereomeric enzyme–substrate complexes were run and compared by several geometric descriptors (all descriptors considered can be found in the Supporting Information). No single descriptor was able to give a complete explanation of the selectivity, so we evaluated all substrates separately to identify the vital interactions. There are two key descriptors that were found to be of great importance. One is the catalytic hydrogen bond distance D1 from the substrate alcohol to His224, and the other is the torsion angle T1 (Figure 2). For a reactive geometry, T1 should have a value close to zero. This is because of the possibility of stabilizing a nucleophilic attack of an incoming alcohol. Torsion T1 also dictates the substrate interaction with the medium pocket; torsions close to zero orient the substrate down into the stereospecificity pocket and are thus found to enhance enantiorecognition. The less reactive substrates exhibited unfavorable interactions, indicated by higher torsion values. For the substrates with high T1 torsion values, we observed that the chiral centers in the 2-position are elevated slightly in order to provide better interaction between the methyl group and the medium pocket.

Secondary alcohols with aliphatic side chains

Unfunctionalized secondary alcohols are known to be acetylated by CALB with very high enantioselectivity (*E* values over 300).[21] The *R* enantiomer of, for example, hexan-2-ol is able to maintain a relaxed conformation with the methyl group pointing into the medium stereospecificity pocket. For the corresponding *S* enantiomer we observed that a twisted conformation was needed to keep the methyl group in place. This twisted conformation relaxes through breakage of the vital hydrogen bond to His224 (Figure 3) during the time course of the MD simulation (Figure 4). The internal energies of the substrate confirm that a higher-energy conformation is needed for the *S* enantiomer to retain the hydrogen bond. This energy is released when the hydrogen bond is broken (Figure 4).

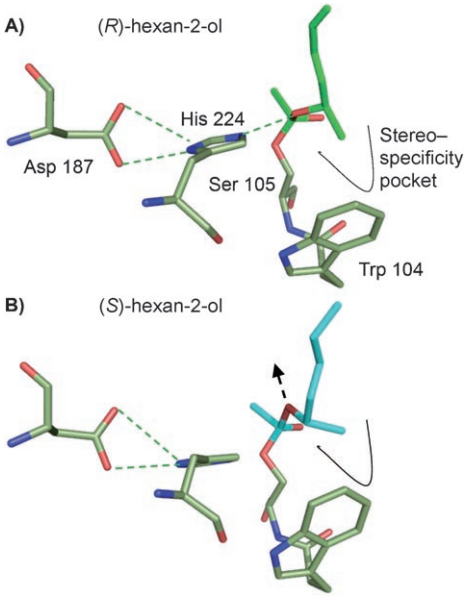

Figure 3. A) (*R*)-Hexan-2-ol shows an ideal catalytic conformation in which the hydrogen bond to His224 is retained during the simulation and the methyl group points towards Trp104. B) In the case of (*S*)-hexan-2-ol the hydrogen bond is broken when the oxygen is twisted upward.

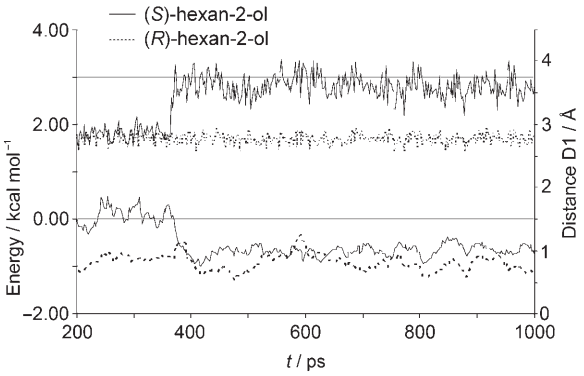

Figure 4. Top: Hydrogen bond distance between the substrate alcohol and His224. A clear break in the distance can be spotted after 400 ps, indicating that the hydrogen bond is broken in the case of (*S*)-hexan-2-ol. The hydrogen bond in (*R*)-hexan-2-ol is kept constant during the complete dynamics. Bottom: Internal energies for the two substrate monomers. The higher energy for (*S*)-hexan-2-ol is released when the hydrogen bond to His224 is broken.

Secondary alcohols containing a δ-alcohol functionality

The modeled alcohol hexane-2,5-diol (**5**) has three different isomers: (*R*,*R*)-**5**, (*S*,*S*)-**5**, and *meso*-**5**. The last of these can be acylated by the enzyme either at the *R* secondary alcohol or at the *S* secondary alcohol. Therefore, diol *meso*-**5** can form two different tetrahedral intermediates, one at the *R* alcohol and the other at the *S* alcohol. The interaction of the alcohol bound to the enzyme resembles that of hexan-2-ol in the simulation, but the δ-hydroxy group forms an additional hydrogen bond with the backbone carbonyl group of Thr40. All four interactions lead to similar binding conformations. Figure 5B shows two tetrahedral intermediates—(*R*)-bound *meso*-**5** and (*S*,*S*)-**5**—but the other two intermediates—(*R*,*R*)-**5** and (*S*)-bound *meso*-**5**—are very similar: (*R*,*R*)-**5** resembles (*R*)-bound *meso*-**5**, and (*S*)-bound *meso*-**5** resembles (*S*,*S*)-**5**. The conformation with hydrogen-bonded δ-alcohol is retained during the complete dynamics, indicating the importance of this interaction. The *S* secondary alcohol groups (that is, those in (*S*,*S*)-**5** and *meso*-**5**) are held in place in spite of the unfavorable interaction in the 2-position, unlike in the case of (*S*)-hexan-2-ol, in which the hydrogen bond to His224 was broken and the catalytic conformation was lost. When the configuration of the alcohol to be acylated is *R*, the tetrahedral intermediates are in a more relaxed conformation than those formed from the *S* alcohol. Interestingly, there is no measurable difference between the tetrahedral intermediate formed from (*R*,*R*)-**5** and the tetrahedral intermediate formed from the *R* alcohol of *meso*-**5** (compare entries 3 and 5, Table 1). A possible explanation might be that there is no large difference in steric bulk when the δ-stereocenter is changed, due to the limited size of the alcohol group. Thus, regardless of the stereochemistry of the δ-alcohol, both substrates can form hydrogen bonds to Thr40, which rigidifies the substrates. A greater difference was observed for the tetrahedral intermediates formed from (*S*,*S*)-**5** and from the *S* alcohol from *meso*-**5** (compare entries 4 and 6, Table 1). The increased difference reflects the unfavorable interaction between the 2-methyl group and the medium selectivity pocket. We therefore conclude that the δ-stereocenters are involved in similar interactions for all investigated diols and that enantioselectivity is dependent on the relative stereochemistry in the 2-positions, where the *R* configuration is favored.

Secondary alcohols with δ-acetate functionality

If an acetoxy group is introduced at the δ-position, the energy differences associated with the different orientations due to stereochemistry are considerably increased. In the active site of CALB there are no hydrogen bond donors present that could orient the ester group. All acetate substituents were found to be positioned in a small polar cavity in the large binding pocket formed by the side chain and the backbone of Ala281 and Ala282. Figure 5C shows two tetrahedral intermediates: (*R*,*R*)-**6** and (*S*,*S*)-**6**. A favorable electrostatic interaction between the ester carbonyl oxygen and the peptide NH of Ala282 could be identified for (*R*,*R*)-**6**, but with (*S*,*S*)-**6** no such interaction is possible (Figure 5C). From this observation and from the determination of a higher T1 torsion value for (*S*,*S*)-**6**

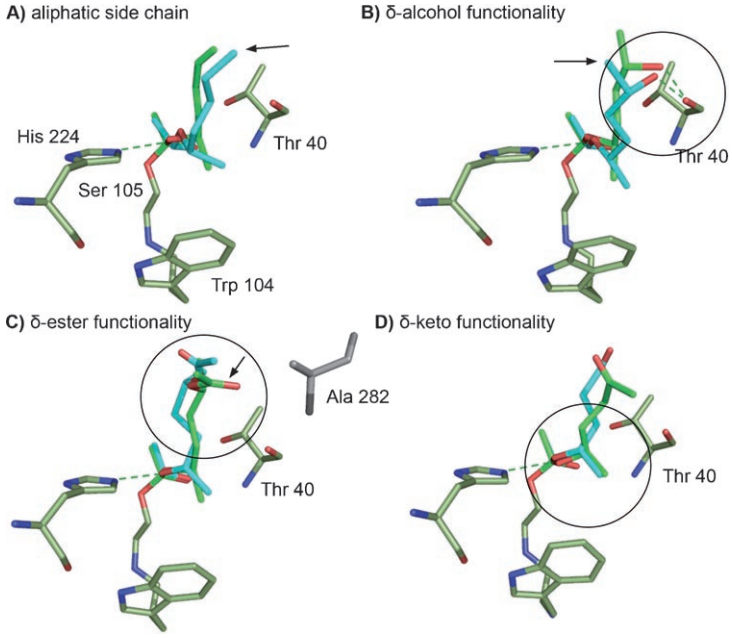

Figure 5. A) (*R*)-Hexan-2-ol is in an ideal conformation, whereas (*S*)-hexan-2-ol (indicated by the arrow) adopts a twisted non-catalytic conformation. B) Thr40 forms a hydrogen bond to the δ-hydroxy group on all substrates: (*S*,*S*)-**5** (arrow) and *R*-bound *meso*-**5** are shown. In the (*S*,*S*)-**5** case, it can be observed that the (2*S*) configuration enforces deviation of the planar torsion T1, indicating a more slowly reacting substrate. C) Diol monoacetate (*R*,*R*)-**6** (arrow) aligns the carbonyl group towards the peptide NH of Ala282, where stabilization by hydrogen bonding can occur. This conformation is not accessible to (*S*,*S*)-**6**. This can explain the enzyme preference for the δ-*R* acetates. D) With a keto group in the δ-position, the *R* and the *S* enantiomer both adopt a similar binding mode in which the methyl group is elevated because of the electrostatic repulsion to Thr40. The enantiorecognition by the selectivity pocket at Trp104 is lost.

Table 1. Results from the MD simulations.

	Substrate	Distance D1 [Å]	Torsion T1 [°]	*E* value[a]
1	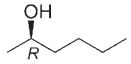 (*R*)-hexan-2-ol	2.8±0.1	0±20	>300
2	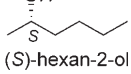 (*S*)-hexan-2-ol	3.6±0.3	−88±18	
3	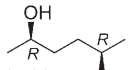 (*R*,*R*)-**5**	2.8±0.1	−4±12	>200
4	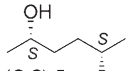 (*S*,*S*)-**5**	2.7±0.1	15±28	
5[b]	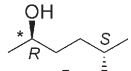 *meso*-**5**	2.8±0.1	−6±12	>200
6[b]	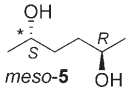 *meso*-**5**	2.8±0.1	0±21	
7	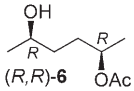 (*R*,*R*)-**6**	2.8±0.1	3±14	94
8	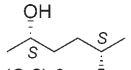 (*S*,*S*)-**6**	2.7±0.1	26±14	
9	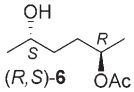 (*R*,*S*)-**6**	2.7±0.1	9±22	7
10	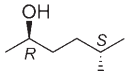 *ent*-(*R*,*S*)-**6**	2.8±0.1	14±19	
11	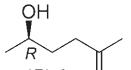 (*R*)-**3**	2.8±0.1	19±16	9
12	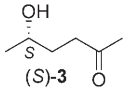 (*S*)-**3**	2.7±0.1	21±14	

[a] Experimentally determined *E* values. [b] The alcohol to be acylated by the enzyme is shown with an asterisk.

than for (*R*,*R*)-**6** (entries 7 and 8, Table 1), a disfavored reaction for the former enantiomer is predicted. For the tetrahedral intermediate originating from (*R*,*S*)-**6** (monoacetate with acetate in the *R* configuration; see the Supporting Information) there will be an interaction with Ala282. To isolate the impact from the remote group in the δ-position, we compared monoacetate (*R*,*R*)-**6** with *ent*-(*R*,*S*)-**6**. In this case, we observed a lower dihedral angle T1 for (*R*,*R*)-**6** (3° vs. 14°; compare entries 7 and 10 in Table 1), and also a smaller difference between them (compare entries 7 and 10, Table 1). The T1 torsion for (*R*,*S*)-**6** (Table 1, entry 9) indicates a higher reactivity. This could explain the experimentally observed low enantioselectivity in the kinetic resolution of a racemic mixture of (*R*,*S*)-**6** and *ent*-(*R*,*S*)-**6** (Figure 1). The disfavored interaction with the (2*S*)-alcohol is compensated by a favorable δ-interaction. We therefore conclude that the presence of an *R* or *S* acetate in the δ-position has an additional effect on the stereoselectivity, and that CALB favors monoacetates that have the δ-acetate in the *R* configuration.

Secondary alcohols with δ-keto functionality

When a keto group is present in the δ-position, the enzyme loses almost all of its selectivity (Scheme 3). During the MD simulation and in an additional systematic conformational search, no conformation stabilized through hydrogen bonding inside the binding pocket could be found. Instead, we found a new binding mode in which the substrate is slightly elevated from the active site (Figure 5D). The elevated binding mode can be observed in the high T1 torsion values observed for both enantiomers (19° and 21°), and the similarities of these values indicate that the two enantiomers have similar binding conformations. We believe that this binding mode is due to electrostatic repulsion between the δ-keto group of the substrate and the Thr40 carbonyl group. While elevated, the interaction between the methyl group and the stereospecificity pocket at Trp104 cannot be maintained by either the *R* or the *S* enantiomer. The substrate can sacrifice this interaction of the 2-methyl group in order to compensate for the repulsion forces. We thus conclude that the δ-keto functionality enforces a nondiscriminating conformation in the active site pocket.

The presence of a keto group in the δ-position results in the sp^2-hybridized carbon being two bonds closer to the active site than in the case of the presence of an acetate. This situation could have further impact on the observed binding mode.

On the basis of this hypothesis, we propose that a water molecule bridging the δ-keto group with the backbone carbonyl of Thr40 should be able to restore the selectivity. We constrained the water molecule to keep its hydrogen bond with Thr40 and monitored the hydrogen bond with the δ-keto substrate. In a second simulation, we introduced a hydrogen bond donor into the enzyme by computationally mutating alanine in position 281 to serine. Ala281 is located in the large binding pocket close to the δ-position (Figure 2). The results of these simulations are reported in Table 2, and a picture of the geometries observed can be found in the Supporting Information. Indeed, simulations with a water molecule placed manually next to Thr40 indicated that this additional hydrogen bond could induce enantiodiscrimination by bringing the stereocenter back into contact with the stereospecificity pocket. We observed a difference of about 60° in favor of the *R* enantiomer in the torsion angle T1 of the δ-keto substrate. Although the hydrogen bond distance remains unchanged, this change in torsion would probably weaken the hydrogen bond to His224, as observed for the diols and the monoacetates. The introduction of a hydrogen bond donor in position 281 through an Ala281Ser mutation gave results comparable with the hexan-2-ol case. Both descriptors—hydrogen bond distance and torsion angle T1—are ideal for the *R* enantiomer but less favorable for the *S* enantiomer.

Table 2. Simulation of two modifications that might increase enantioselectivity with keto-containing substrates.

	Substrate	Simulation	D1 [Å]	D2 [Å][a]	T1 [°]
1	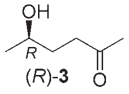 (*R*)-**3**	Ala281Ser	2.8±0.1	3.2±0.5	5±20
2	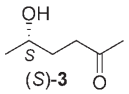 (*S*)-**3**	Ala281Ser	3.6±0.2	3.0±0.3	−90±13
3	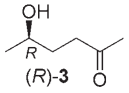 (*R*)-**3**	water	2.8±0.1	3.0±0.2	−4±13
4	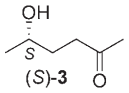 (*S*)-**3**	water	2.8±0.1	3.0±0.2	59±42

[a] Distance between the substrate keto group and the H-bond donor.

The suggested Ala281Ser mutant was produced by site-directed mutagenesis (procedures for the mutagenesis can be found in the Supporting Information), and the enantioselectivity of the mutant in kinetic resolution of **3** was measured in a similar way to that previously described.[12c] The *E* value of the mutant Ala281Ser obtained in enzymatic acylation of **3** was 120 (see the Supporting Information). This shows that a high enantioselectivity for enzymatic acylation of keto alcohol **3** is obtained by replacing alanine with serine in position 281 in CALB, as predicted by the modeling. Further studies of this mutant, to determine its scope and limitations in kinetic resolution of other δ-keto alcohols, are ongoing in our research group.

Conclusions

We have investigated the enantioselectivity of CALB towards several δ-functionalized secondary alcohols by MD simulations. The conclusion from our study is that the enantioselectivity seems to be greatly influenced by the interaction between the functional group in the δ-position and the surrounding enzyme. We found the interaction with Thr40 to be especially important. The Thr40 backbone carbonyl group introduces a small polar environment close to the oxyanion hole that gives rise to electrostatic interactions between the substrate and the enzyme. In the case of diols, this interaction consists of a stabilizing hydrogen bond that rigidifies the investigated substrate, and the selectivity is only dependent on the configuration of the 2-methyl group. The binding situation for the monoacetates differs from that of the diols in one key aspect; the δ-acetate has no hydrogen bond donor. Instead, we found all ester moieties to be located in a cavity between Ala281 and Ala282 at the upper rim of the large binding pocket. In our model the δ-(*R*)-monoacetates are favored through an electrostatic interaction of the carbonyl, in the acetyl group, and the NH group of Ala282. With a keto group in the δ-position, we could only find repulsive interaction with the backbone, favoring a non-discriminating binding mode.

Our current model is qualitatively able to describe the enantioselectivity of a series of δ-substituted secondary alcohols on the basis of geometric properties of their tetrahedral intermediates. Understanding of the interaction of δ-functionalities might help us to identify problematic substrates in advance and, by protein engineering, to expand the scope of biocatalysis.

Experimental Section

Preparation of the enzyme model: The enzyme model is based on the 1TCA[7] crystal structure of CALB. Excess water molecules and water molecules in the active site were removed, and only conserved backbone bridging water molecules were left in the structure. Possible errors in the X-ray structure were investigated with the aid of the WHAT_CHECK[22] routine. Asp134 was protonated because of its predicted high pK_a (7.18)[23] and its location close to the catalytic Asp187. The prepared monomeric enzyme structure was initially minimized to remove any large gradients and then equilibrated by MD at 300 K. All substrates were modeled as their tetrahedral intermediates covalently bound to the enzyme. The lipase mechanism has been reviewed by Ema,[24] and the nucleophilic attack of the free alcohol on the acyl enzyme to form a tetrahedral intermediate is the overall rate-limiting step of the reaction in most cases.[18,25] The transition states in enantioselective serine hydrolase catalysis are known from some recent QM studies in the gas phase[26] and from QM/MM[18,25] to be geometrically and energetically closely related to the tetrahedral intermediates, and this supports the validity of our chosen modeling approach.

Computational methods: All MD simulations were performed with the Moloc computational package and the MAB force field[27] (MAB mask used: 928, preserve stereocenter conformation, preserve *cis-trans* conformation, ignore hydrogen bond between fixed atoms and hydrogen bond scale for vacuum). Several individual 1 ns MD simulations at 300 K were run for each substrate with use of Langevin-type dynamics and a step size of 2 fs. Coordinates were sampled every 2 ps, leading to 500 individual structures per trajectory. All descriptors were analyzed after an equilibration phase of 200 ps with use of statistical median values. Solvation effects were simulated by adding discrete toluene molecules in a half-sphere of 20 Å around all flexible parts of the enzyme. The advantage of the chosen MAB force field is an extensively parameterized united atom approach that is capable of modeling both the substrates and the toluene molecules explicitly. It has been shown that the MAB force field is able to describe lipase tetrahedral intermediates equally well as CHARMM[11] or AMBER[16] simulations. General force field errors are expected to be in the range of 1–2 kcal mol^{-1}, which makes absolute determination of the *E* value impossible,[28] and allows only semiquantitative evaluations, as the *E* value range of 20 to 200 represents energy differences of about 2–4 kcal mol^{-1}.

(*R*)-5-Phenylpentan-2-ol was modeled into the active site, and a reaction sphere of 10 Å around the monomer was chosen and used for all substrates. Substrates were modeled with crystal structures of CALB with (*R*)- and (*S*)-phenylethylamine-phosphonates as reference.[11] The binding mode was chosen so that all hydrogen bonds were present. Stereospecificity pockets described as large refer to the enzyme entrance pocket, medium to the pocket limited by Trp104, and small to the pocket that is found next to the oxyanion

hole near Thr40, in which the α-hydrogen at the stereocenter preferentially resides (Figure 2).

The experimental reactions were performed in toluene as the solvent. Standard biomolecular modeling approaches are parameterized specially for aqueous solvents with use either of implicit solvation or of explicit TIP- or SPC-water models. Modeling of enzyme reactions in organic solvents therefore requires either the approximation of the hydrophobic solvent as a vacuum or a customized parameterization of the solvent. For the CHARMM force field no equilibrated boxes for non-aqueous solvents are published, whereas for the AMBER parm99 force field, some organic solvents such as DMSO, methanol, acetonitrile, or chloroalkyls[29] are available for condensed phase simulations and were used for studies on lid movement in the case of Crl.[30] Because CALB does not show structural changes when a substrate is coordinated[8] and does not contain a large lid helix, we believed that it should behave more like subtilisin Carlsberg, where the enzyme structure remained largely unchanged when the crystal was soaked with organic solvents.[31] The use of molecular modeling approaches for enzymes in organic solvent has been reviewed by Carrea.[32] For the force field used in this study, an implicit water model and a vacuum model with adapted hydrogen bond strengths for vacuum simulations are available. When comparing the three solvation models—the two available in the force field and the discrete toluene cap (data not shown)—we found that the full approach with explicit solvent molecules was able to decrease the motion of the substrate in the active site and therefore gave more consistent trajectories. We thus concluded that the choice of solvation model is important for reliable modeling of enzyme reactions in organic solvents.

Acknowledgements

Financial support from the Swedish Research Council, the Swedish Foundation for Strategic Research, and the K&A Wallenberg Foundation is gratefully acknowledged. We thank Dr. Alex Kasrayan for providing us with the CALB pPICZ vector.

Keywords: bioorganic chemistry · C*andida antarctica* lipase B · molecular dynamics · molecular modeling · organic chemistry

[1] A. M. Rouhi, *Chem. Eng. News* **2004**, *82*, 47–62.
[2] a) J. Halpern, B. M. Trost, *Proc. Natl. Acad. Sci. USA* **2004**, *101*, 5347; b) I. Ojima, *Catalytic Asymmetric Synthesis*, 2nd ed., Wiley-VCH, New York, **2000**; c) E. N. Jacobsen, A. Pfaltz, H. Yamamoto, *Comprehensive Asymmetric Catalysis*, Springer, Berlin, **1999**; d) R. Noyori, *Asymmetric Catalysis in Organic Synthesis*, Wiley, New York, **1994**; e) K. Drauz, H. Waldmann, *Enzyme Catalysis in Organic Synthesis: A Comprehensive Handbook, Vols. I–III*, 2nd ed., Wiley-VCH, Weinheim, **2002**f) K. Faber, *Biotransformations in Organic Chemistry*, 4th ed., Springer, Berlin, **2000**; g) P. I. Dalko, L. Moisan, *Angew. Chem.* **2004**, *116*, 5248–5286; *Angew. Chem. Int. Ed.* **2004**, *43*, 5138–5175.
[3] M. Breuer, K. Ditrich, T. Habicher, B. Hauer, M. Keβeler, R. Stürmer, T. Zelinski, *Angew. Chem.* **2004**, *116*, 806–843; *Angew. Chem. Int. Ed.* **2004**, *43*, 788–824.
[4] E. L. Eliel, S. H. Wilen, L. N. Mander, *Stereochemistry of Organic Compounds*, Wiley, New York, **1994**.
[5] R. J. Kazlauskas, A. N. E. Weissfloch, A. T. Rappaport, L. A. Cuccia, *J. Org. Chem.* **1991**, *56*, 2656–2665; *R* and *S* selectivity are used for typical *sec*-alcohols in which the large group has the higher priority in the sequential rule for determining the configuration according to the Cahn–Ingold–Prelog system.
[6] a) L. Brady, A. M. Brzozowski, Z. S. Derewenda, E. Dodson, G. Dodson, S. Tolley, J. P. Turkenburg, L. Christiansen, B. Huge-Jensen, L. Norskov, L. Thim, U. Menge, *Nature* **1990**, *343*, 767–770; b) M. Martinelle, K. Hult, *Biochim. Biophys. Acta* **1995**, *1251*, 191–197; c) J. Kraut, *Annu. Rev. Biochem.* **1977**, *46*, 331–358.
[7] J. Uppenberg, M. T. Hansen, S. Patkar, T. A. Jones, *Structure* **1994**, *2*, 293–308.
[8] J. Uppenberg, N. Öhrner, M. Norin, K. Hult, G. J. Kleywegt, S. Patkar, V. Waagen, T. Anthonsen, T. A. Jones, *Biochemistry* **1995**, *34*, 16838–16851.
[9] F. Hæffner, T. Norin, K. Hult, *Biophys. J.* **1998**, *74*, 1251–1252.
[10] a) S. Raza, L. Fransson, K. Hult, *Protein Sci.* **2001**, *10*, 329–338; b) J. Ottosson, L. Fransson, K. Hult, *Protein Sci.* **2002**, *11*, 1462–1471.
[11] M. Bocola, M. T. Stubbs, C. Sotriffer, B. Hauer, T. Friedrich, K. Dittrich, G. Klebe, *Protein Eng.* **2003**, *16*, 319–322.
[12] a) M. Edin, J.-E. Bäckvall, *J. Org. Chem.* **2003**, *68*, 2216–2222; b) B. Martin-Matute, J.-E. Bäckvall, *J. Org. Chem.* **2004**, *69*, 9191–9195; c) B. Martín-Matute, M. Edin, J.-E. Bäckvall, *Chem. Eur. J.* **2006**, *12*, 6053–6061.
[13] For examples, see: C. Orrenius, N. Ohrner, D. Rotticci, A. Mattson, K. Hult, T. Norin, *Tetrahedron: Asymmetry* **1995**, *6*, 1217–1220.
[14] a) Z. W. Guo, S. H. Wu, C. S. Chen, G. Girdaukas, C. J. Sih, *J. Am. Chem. Soc.* **1990**, *112*, 4942–4945; b) A. Mattson, N. Öhrner, K. Hult, T. Norin, *Tetrahedron: Asymmetry* **1993**, *4*, 925–930; c) G. Caron, R. J. Kazlauskas, *Tetrahedron: Asymmetry* **1994**, *5*, 657–664; d) For related studies on 3-hydroxy esters in organic solvents, see: U. Bornscheuer, A. Herar, L. Kreye, V. Wendel, A. Capewell, H. H. Meyer, T. Scheper, F. N. Kolisis, *Tetrahedron: Asymmetry* **1993**, *4*, 1007–1016.
[15] The *E* value (enantiomeric ratio) is applied only to enantiomers. In this case, the starting substrate is a mixture of *rac*/diastereomeric diols. It was found that the stereochemistry of the inner alcohol does not affect the enzyme-catalyzed acetylation of the less hindered alcohol. The measured kinetic parameter was called the pseudo *E* value.
[16] M. Bocola, N. Otte, K.-E. Jaeger, M. T. Reetz, W. Thiel, *ChemBioChem* **2004**, *5*, 214–223.
[17] T. Schulz, J. Pleiss, R. D. Schmid, *Protein Sci.* **2000**, *9*, 1053–1062.
[18] S. A. Funke, N. Otte, T. Eggert, M. Bocola, K.-E. Jaeger, W. Thiel, *Protein Eng. Des. Sel.* **2005**, *18*, 509–514.
[19] A. Magnusson, K. Hult, M. Holmquist, *J. Am. Chem. Soc.* **2001**, *123*, 4354–4355.
[20] A. Mezzetti, J. D. Schrag, C. S. Cheong, R. J. Kazlauskas, *Chem. Biol.* **2005**, *12*, 427–437.
[21] S. Patkar, J. Vind, E. Kelstrup, M. W. Christensen, A. Svendsen, K. Borch, O. Kirk, *Chem. Phys. Lipids* **1998**, *93*, 95–101.
[22] R. W. W. Hooft, G. Vriend, C. Sander, E. E. Abola, *Nature* **1996**, *381*, 272–272.
[23] H. Li, A. D. Robertson, J. H. Jensen, *Proteins Struct. Funct. Bioinf.* **2005**, *61*, 704–721.
[24] T. Ema, *Curr. Org. Chem.* **2004**, *8*, 1009–1025.
[25] a) M. Topf, P. Várnai, W. G. Richards, *J. Am. Chem. Soc.* **2002**, *124*, 14780–14788; b) V. Daggett, S. Schröder, P. Kollman, *J. Am. Chem. Soc.* **1991**, *113*, 8926–8935.
[26] a) S. Tomic, M. Ramek, *J. Mol. Catal. B* **2006**, *38*, 139–147; b) L. De Santis, P. Carloni, *Proteins Struct. Funct. Bioinf.* **1999**, *37*, 611–618; c) C.-H. Hu, T. Brinck, K. Hult, *Int. J. Quantum Chem.* **1998**, *69*, 89–103.
[27] P. R. Gerber, *J. Comput.-Aided Mol. Des.* **1998**, *12*, 37–51.
[28] R. J. Kazlauskas, *Curr. Opin. Chem. Biol.* **2000**, *4*, 81–88.
[29] T. Fox, P. A. Kollman, *J. Phys. Chem. B* **1998**, *102*, 8070–8079.
[30] B. A. Tejo, A. B. Salleh, J. Pleiss, *J. Mol. Model.* **2004**, *10*, 358–366.
[31] J. L. Schmitke, L. J. Stern, A. M. Klibanov, *Proc. Natl. Acad. Sci. USA* **1997**, *94*, 4250–4255.
[32] G. Colombo, G. Ottolina, G. Carrea, *Monatsh. Chem.* **2000**, *131*, 527–547.

Received: January 18, 2008
Published online on July 24, 2008

